Received: 17 May 2022 | Revised: 9 August 2022 | Accepted: 4 September 2022

DOI: 10.1111/omi.12389

ORIGINAL ARTICLE

WILEY

Oral biofilm dysbiosis during experimental periodontitis

Apoena Aguiar Ribeiro[1] | Yizu Jiao[2] | Mustafa Girnary[2] | Tomaz Alves[2] | Liang Chen[2] | Anna Farrell[1] | Di Wu[3,4] | Flavia Teles[5] | Naohiro Inohara[6] | Karen V. Swanson[7] | Julie T. Marchesan[2]

[1]Division of Diagnostic Sciences (Microbiology and Cariology), Adams School of Dentistry, University of North Carolina at Chapel Hill, Chapel Hill, North Carolina, USA

[2]Division of Comprehensive Oral Health (Periodontology), Adams School of Dentistry, University of North Carolina at Chapel Hill, Chapel Hill, North Carolina, USA

[3]Division of Oral and Craniofacial Health Sciences, Adams School of Dentistry, University of North Carolina at Chapel Hill, Chapel Hill, North Carolina, USA

[4]Department of Biostatistics, Gillings School of Global Public Health, University of North Carolina at Chapel Hill, Chapel Hill, North Carolina, USA

[5]Department of Basic and Translational Sciences, Penn Dental Medicine, University of Pennsylvania, Philadelphia, Pennsylvania, USA

[6]Department of Pathology, Michigan Medicine, University of Michigan, Ann Arbor, Michigan, USA

[7]Division of Infectious Diseases, School of Medicine, University of North Carolina at Chapel Hill, Chapel Hill, North Carolina, USA

Correspondence
Julie Marchesan, Division of Comprehensive Oral Health (Periodontology), Adams School of Dentistry, University of North Carolina at Chapel Hill, 3506 Koury Oral Health Sciences Building, Chapel Hill, NC 27599, USA.
Email: julie_marchesan@unc.edu

Funding information
National Institutes of Health; National Institute of Dental and Craniofacial Research; Coordenação de Aperfeiçoamento de Pessoal de Nível Superior

Abstract

Objectives: We have previously characterized the main osteoimmunological events that occur during ligature periodontitis. This study aims to determine the polymicrobial community shifts that occur during disease development.

Methods: Periodontitis was induced in C57BL/6 mice using the ligature-induced periodontitis model. Healthy oral mucosa swabs and ligatures were collected every 3 days from 0 to 18 days post-ligature placement. Biofilm samples were evaluated by 16SrRNA gene sequencing (Illumina MiSeq) and QIIME. Time-course changes were determined by relative abundance, diversity, and rank analyses (PERMANOVA, Bonferroni-adjusted).

Results: Microbial differences between health and periodontal inflammation were observed at all phylogenic levels. An evident microbial community shift occurred in 25 genera during the advancement of "gingivitis" (3–6 days) to periodontitis (9–18 days). From day 0 to 18, dramatic changes were identified in *Streptococcus* levels, with an overall decrease (54.04%–0.02%) as well an overall increase of *Enterococcus* and *Lactobacillus* (23.7%–73.1% and 10.1%–70.2%, respectively). Alpha-diversity decreased to its lowest at 3 days, followed by an increase in diversity as disease advancement. Beta-diversity increased after ligature placement, indicating that bone loss develops in response to a greater microbial variability ($p = 0.001$). Levels of facultative and strict anaerobic bacteria augmented over the course of disease progression, with a total of eight species significantly different during the 18-day period.

Conclusion: The data supports that murine gingival inflammation and alveolar bone loss develop in response to microbiome shifts. Bacterial diversity increased during progression to bone loss. These findings further support the utilization of the periodontitis ligature model for microbial shift analysis under different experimental conditions.

KEYWORDS
biofilm, dysbiosis, experimental periodontitis

Abbreviations: OTU, operational taxonomic unit; PCoA, Principal Coordinate Analysis.

© 2022 John Wiley & Sons A/S. Published by John Wiley & Sons Ltd.

1 | INTRODUCTION

Periodontitis is an inflammatory disease caused by a dysbiotic microbiota (Abe, Hajishengallis, 2013). The dysbiosis is characterized by the microbial shift that occurs in the biofilm with a decrease in the number of beneficial symbionts and/or an increase in the number of pathobionts, as microorganisms become pathogenic when host–microbe homeostasis breaks down (Hajishengallis, Lamont, 2016; Jiao et al., 2013). The polymicrobial community shift induces a host response that results in the destruction of the connective tissue and alveolar bone supporting the tooth. In the clinical setting, individuals with periodontal disease consistently demonstrate a shift in biofilm microbial composition compared to healthy individuals, including increased abundances of certain phylotypes (Paster et al., 2001; Griffen et al., 2012; Paes Batista da Silva et al., 2016; Marchesan et al., 2016).

To better understand the microbial changes and inflammatory host response to these changes, it is important to explore the etiology of periodontitis to improve its treatment. Many host and environmental factors are associated with an oral microbiota dysbiosis, including increased microbial challenge (e.g., biofilm load), smoking, and systemic diseases (Teles et al., 2021; Sanz et al., 2018; Nociti et al., 2015). Although human biofilm samples can be used to characterize the difference between healthy and disease states, dynamic microbial shifts cannot be fully investigated in the clinical setting. Moreover, neither the direct cause nor effect of different host and environmental factors that can directly induce a microbial shift related to disease can be explored in humans. Therefore, experimental animal models are a powerful platform to complement results derived from clinical studies (Hajishengallis et al., 2015).

Different models have been used to study periodontal disease in mice, including the oral gavage, chamber model, and ligature models (Graves et al., 2008). Ligature-induced periodontitis in mice has long served as an animal model for periodontitis. We previously demonstrated that there are distinct osteoimmunological events that developed from health to gingival inflammation and transition to periodontitis at 18 days post-ligature placement (Marchesan et al., 2018). While it is known that bone loss in this model develops in response to bacterial presence, information on the composition and microbial shifts of their oral microbiota is limited. Therefore, the purpose of this study was to expand on our previous immune findings (Marchesan et al., 2018; Swanson et al., 2022) and characterize microbiota changes that occur during periodontitis development in a time-dependent manner. We hypothesized that the ligature placement would be accompanied by time-dependent shift of microorganisms that can be associated with inflammation and periodontal disease development.

2 | METHODS

2.1 | Periodontitis murine model

The protocol was approved by the by University of North Carolina–Chapel Hill Institutional Animal Care and Use Committee and can be observed in Figure 1. Twenty-eight C57BL/6 wild-type, specific pathogen-free female mice aged 8–10 weeks were purchased from Taconic Biosciences. Mice were acclimatized to the animal facility (under pathogen-free conditions) for a period of 7 days upon arrival, and four mice were randomly assigned to one of the groups associated by the time course of the study period. Experimental periodontitis was induced using the ligature model as previously described by our group (Marchesan et al., 2018). Briefly, sterile silk sutures (5-0, SUT-15-1, Roboz Surgical Instrument, Gaithersburg, MD, USA) knotted ~2.5 mm apart were placed between the first and second maxillary molars using a ligature holder, while the mouse was under sedation with isoflurane. Mice were evaluated every 3 days from health (baseline) to 18 days post-ligature placement. Ligature and plaque samples were collected for further analysis in accordance with previous publications (Marchesan et al., 2012, 2013; Jiao et al., 2014). For baseline collection, a sterile swab was placed in the oral cavity of mice and swirled for 15 s before being placed in sterile PBS (Thermo Fisher Scientific, cat. no. 14190144). Tubes were centrifuge for 5 min at 13,000 rpm at 4°C. After centrifugation, PBS was discarded, and samples were stored at −80°C until analysis. At the additional experimental timepoints, ligatures were collected with the usage of a sterile fine-point forceps (Fisher, cat. no. 16-100-113). Collected ligatures were placed in an Eppendorf tube and stored at −80°C. Samples were excluded from the analysis if a ligature was lost before the end point of the experiment. If lost, no ligature was replaced in the mouse to allow the development of a microbial shift. Microbiota analysis was conducted after confirmation of bone destruction by μCT and histological analysis, which was previously conducted and published (Marchesan et al., 2018).

2.2 | DNA isolation and 16s rRNA amplicon library preparation and sequencing

DNA isolation, preparation of sequencing libraries, and sequencing were done in the UNC Microbiome Core Facility as described (Jones et al., 2018). Briefly, bacterial DNA extraction was performed using QIAmp DNA extraction kit (QIAGEN). A step of preincubation with lysozyme for 30 min was introduced to the protocol to ensure optimal DNA yield from gram-positive bacteria. For generation of sequencing libraries, 12.5 ng of total DNA from each sample was amplified using the 2× KAPA HiFi HotStart ReadyMix (KAPA Biosystems, Wilmington, MA). Primers targeting the V3–V4 region of the 16S rRNA gene (Edwards et al., 1989; Thompson et al., 2015) were designed to incorporate Illumina compatible sequencing adaptors. The complete sequences of the primers were as follows: 515 F—5′ TCGTCGGCACGTCAGATGTGTATAAGAGACAGGTGCCAGCMGCCGCGGTAA 3′; 806 R—5′GTCTCGTGGGCTCGGAGATGTGTATAAGAGACAGGGACTACHVGGGTWTCTAAT 3′. PCR conditions consisted of an initial denaturing step at 95°C for 3 min, 25 cycles of 95°C for 30 s, 55°C for 30 s, and 72°C for 30 s, followed by extension at 72°C for 5 min and a final hold at 4°C. Illumina sequencing adapters and dual index barcodes (Illumina, San Diego, CA) were added using one more round

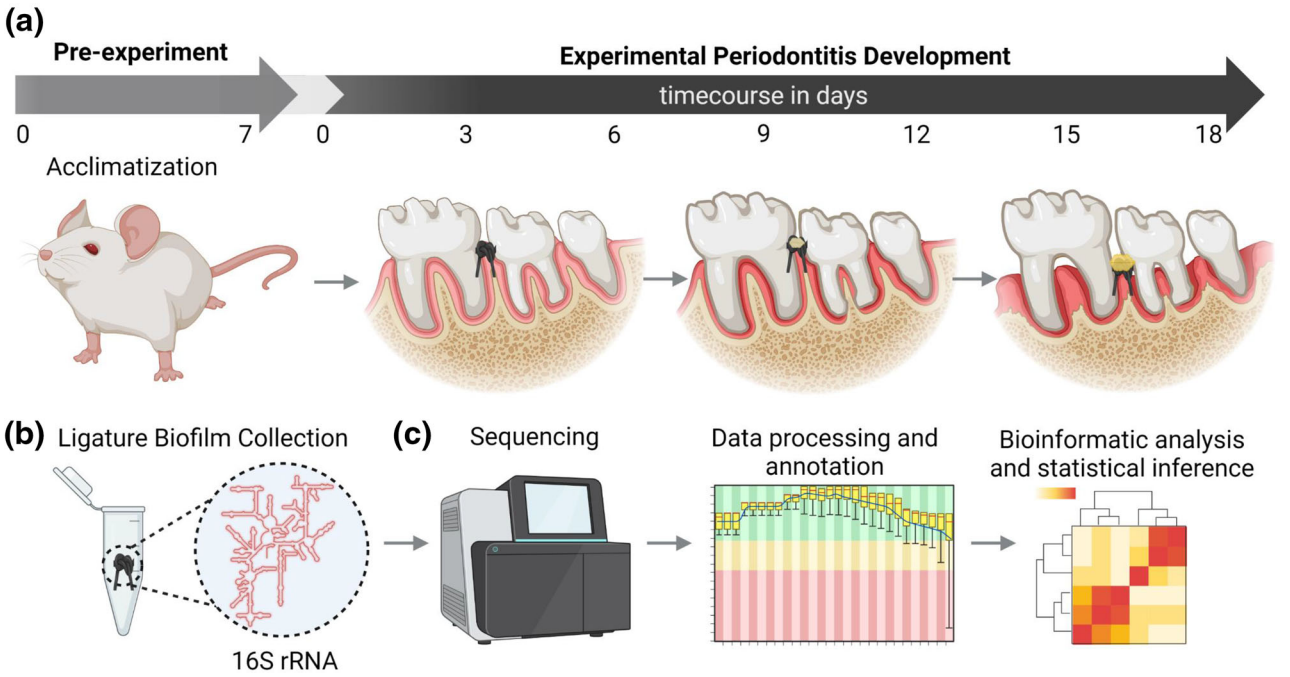

FIGURE 1 Study flowchart of the murine experimental periodontitis induced using the ligature model

of PCR amplification consisting of eight cycles. PCR products were purified using AMPure XP reagent (Beckman Coulter, Indianapolis, IN), quantified by Quanti-IT Picogreen dsDNA 1 kit (Invitrogen), and pooled in equimolar amounts. Sequencing was performed on a MiSeq instrument (Illumina) operating Real Time Analysis software version 1.17.28. Paired-end sequencing used custom primers and a 500-cycle sequencing kit (version 3) according to manufacturer instructions. Amplicon sequencing was carried out in the presence of 7% PhiX control (Illumina) to allow proper focusing and matrix calculations.

2.3 | Bioinformatics pipeline and statistical analysis

Raw sequencing data files were processed using the open-source software pipeline Quantitative Insights into Microbial Ecology (QIIME) version 1.8 (Caporaso et al., 2010). Barcode and primer trimming and sequence quality filtering was performed using QIIME's default script settings. Operational taxonomic units (OTUs) were clustered using QIIME implementation of UCLUST. Taxonomic assignment of OTUs was performed using BLAST against the Greengenes 16S rRNA database. After examining read counts, rarefaction analysis was performed at a sampling depth of 10,000 sequences and rarefaction curves were plotted. Summary of taxonomic assignments was plotted as bar charts using QIIME. Observed species richness, as well as phylogenetic and nonphylogenetic alpha diversity metrics (Chao1 and Shannon's index, respectively), was recorded and compared at the rarefaction depth of 10,000. Phylogenetic and nonphylogenetic beta diversity matrices were calculated by three-dimensional Principal Coordinate Analysis (PCoA) plots, calculated within QIIME using weighted and unweighted UniFrac distances between samples. Statistical analysis was performed with SAS 9.4 software after correction (Bonferroni-adjusted 0.006). The sequencing data will be made available when requested.

Paired *t*-test (within-tooth analysis) was performed to compare alpha diversity. Finally, Benjamini–Hochberg procedure for false discovery rate (Benjamini, Hochberg, 1995) and family-wise error rate (Hochberg, Benjamini, 1990) methods were applied to the *p*-values of the stratified MH mean score statistics for exploratory and confirmatory testing, respectively, to identify any statistically significant differences among genera. An overall error rate of 0.05 was used in each procedure.

3 | RESULTS

After the study period, one sample from time 0 was not included due to low DNA yield, leading to a total of 27 biofilm samples (three samples from baseline and four samples from each group in the time course). A total of 2,856,260 sequences were generated from the 27 biofilm samples, and matched 141 unique species. Amplicon reads with relative abundances higher than 0.01% were assigned to seven bacterial phyla, 19 classes, 33 orders, 45 families, and 113 genera. The most frequent phyla were Bacillota (formerly Firmicutes, relative abundance ranging between 59.7% and 99.8%) and Pseudomonadota (formerly Proteobacteria, relative abundance ranging between 40.2% and 0.05%). Figure 2a shows the 20 most abundant bacterial genera and species profile distribution, according to timepoints, representing between 89% and 99% of the total community. The full list of bacterial samples and its OTUs can be verified in Table S1.

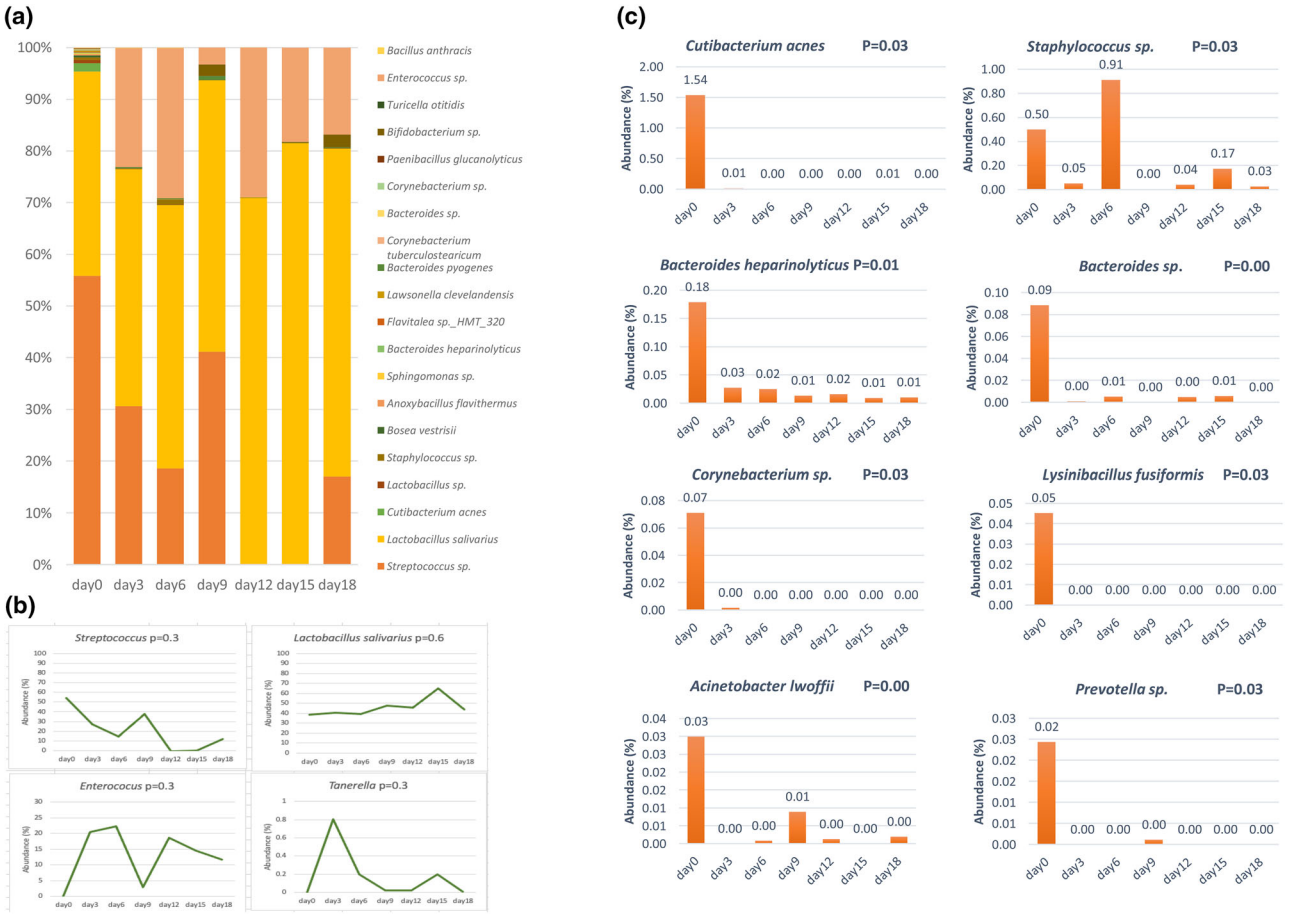

FIGURE 2 Bacterial microbiome composition shifts according to time. (a) Stacked plot for samples' distribution according to time. For illustrations purposes, only the top 20 genera and species are shown in the plot. The community is represented as 99.2% at day 0, 97.9% at day 3, 87.8% at day 6, 93.9% at day 9, 89.8% at day 12, 92% at day 15, and 82.3% at day 18. (b) Relative abundances (%) of *Lactobacillus*, *Streptococcus*, and *Enterococcus* during the time course. (c) Species abundance that significantly changed during the time course (Mantel–Haensel test, $p < 0.05$, Bonferroni corrected)

3.1 | Bacterial microbiome composition shifts according to time

Bacillota encompassed the majority of sequences throughout all time courses, although an increase in Pseudomonadota was observed after 9 days (Figure S1). Among the top 10 most abundant genera, *Lactobacillus*, *Streptococcus*, and *Enterococcus* presented the greatest shifts in abundance during the time course and disease development (Figure 2b). *Tannerella* initially colonized at 3 days with 0.8% of total bacteria, and colonization fell over the 18 days (Figure 2b). The 18-day time course significantly changed the community profile abundances among eight species (Figure 2c). *Cutibacterium acnes*, *Bacteroides* sp., *Bacteroides heparinolyticus*, *Corynebacterium* sp., *Lysinibacillus fusiformis*, *Acinetobacter lwoffii*, and *Prevotella* sp. significantly decreased in abundance associated over the 18-day time course, while *Staphylococcus* sp. became highly abundant by day 6, when compared with the baseline and with the other timepoints. Alpha diversity was highest at health (day 0, pre-ligature), and decreased to its lowest level at the initial phase of disease of 3 days post-ligature placement. This indicates that the microbiome becomes less diverse and, therefore, more specific to the development of periodontal inflammation (Shannon index, paired *t*-test; Figure 3a). The decrease in species diversity within the ligature samples never returned to the baseline levels. PCoA of unweighted UniFrac showed that samples from baseline represented a very distinct community when compared with the other samples, forming a well-defined cluster (Figure 3b), with overall statistically significant differences between the microbiome communities (Pairwise PERMANOVA, $p = 0.001$; Figure 3c). Biofilm community composition from baseline was significantly different when compared to 3 days ($p = 0.04$), 6 days ($p = 0.05$), 12 days ($p = 0.03$), and 15 days ($p = 0.02$). Other significant differences in bacterial beta diversity were found between 3 and 12 days ($p = 0.01$), and between 9 and 12 days ($p = 0.02$).

3.2 | Community shifts associated with disease development

In our previous study, the transition from health to gingival inflammation and no bone loss occurred during the period of 3–6 days, which was dominated by innate immune events (Marchesan et al., 2018).

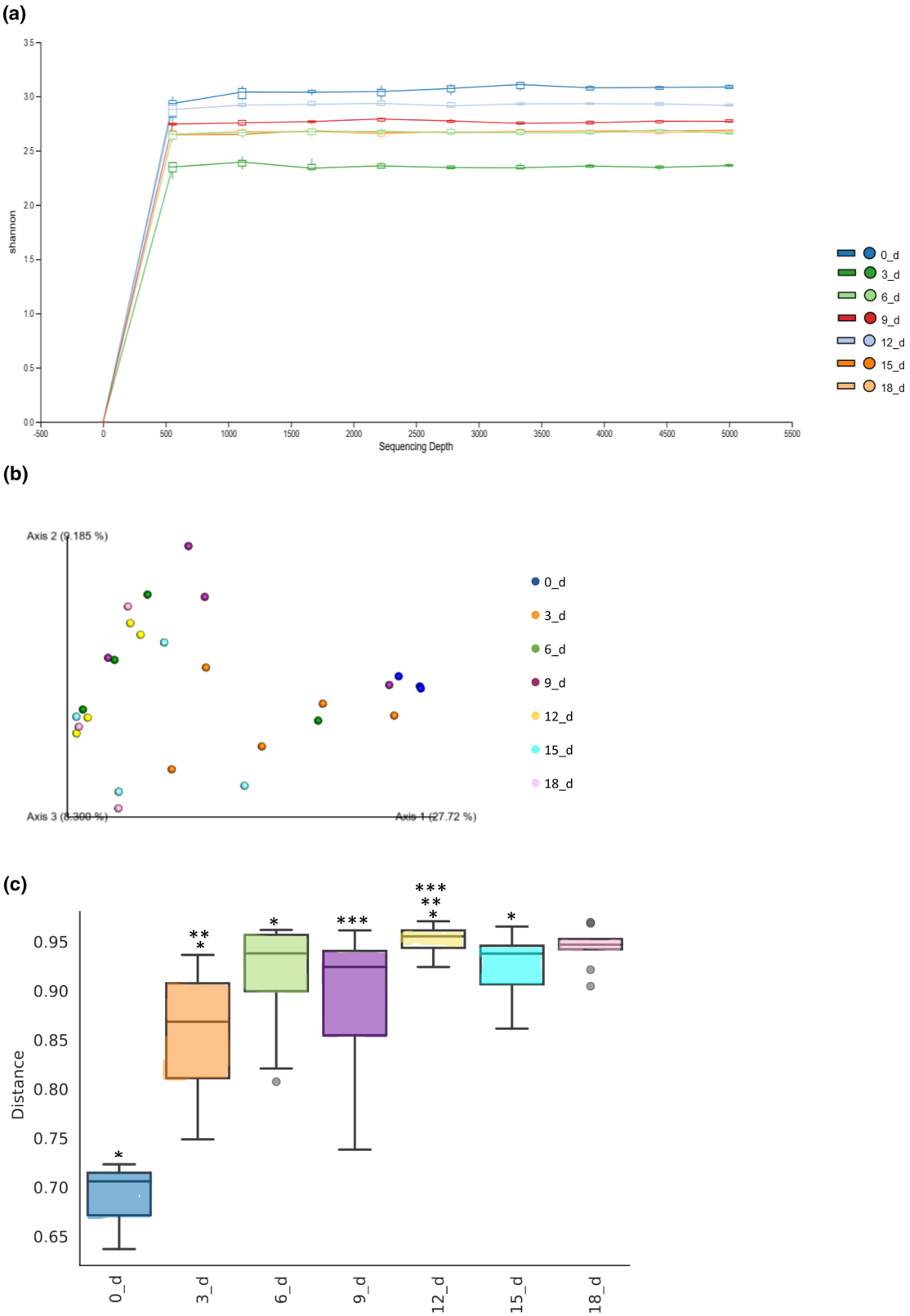

FIGURE 3 Ecological shifts in the microbiome community associated with the length of the ligature presence. (a) Alpha diversity. (b) Unweighted UniFrac Principal Coordinate Analysis (beta diversity) based on time course. (c) Box-plot showing differences between the microbiome communities composition (PERMANOVA, $p = 0.001$)

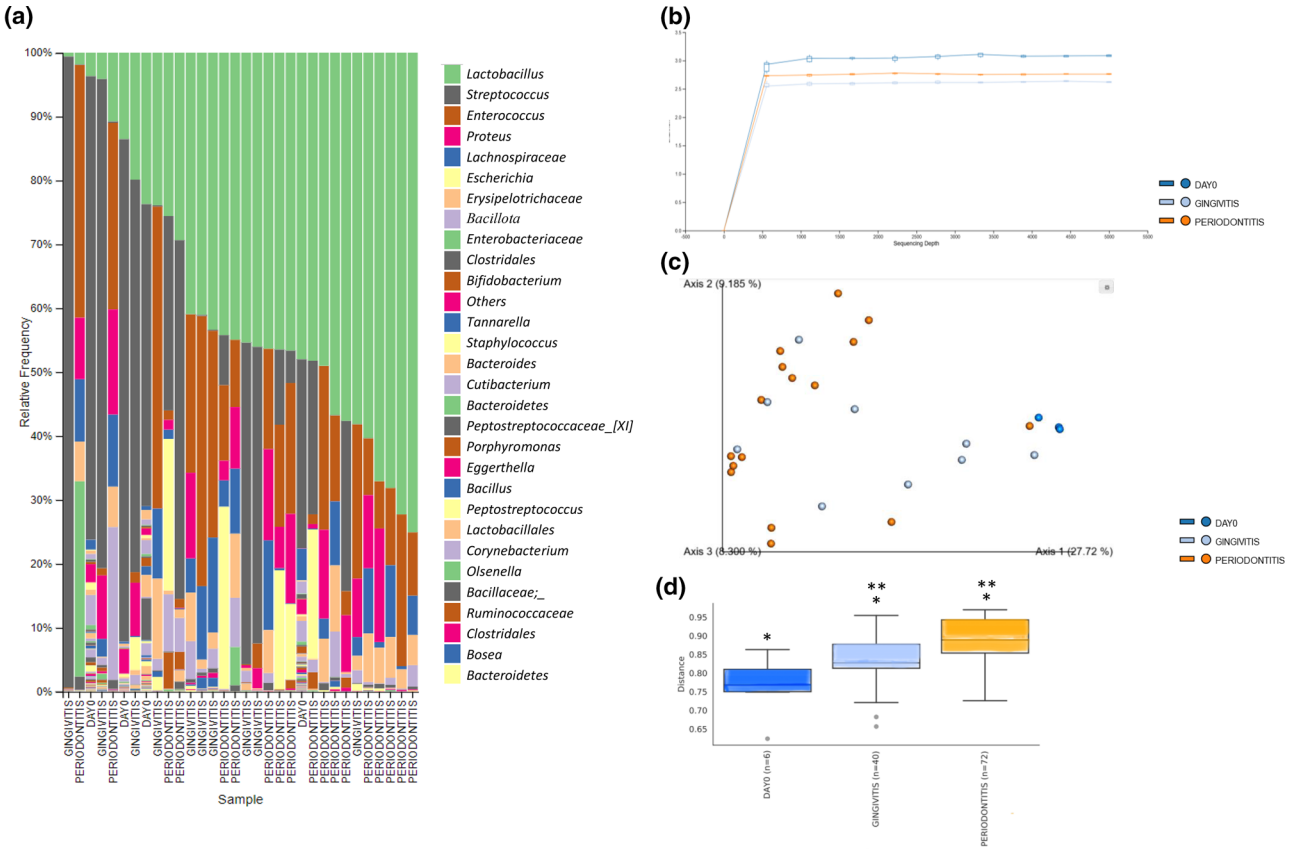

FIGURE 4 Shift of the bacterial microbiome community at genera level, associated with disease development. (a) Stacked plot for samples' distribution according to clinical diagnosis. (b) Shannon index: bacterial diversity decreased within samples during disease development. (c) Unweighted UniFrac Principal Coordinate Analysis (Beta diversity) based on periodontal status. (d) Box-plot showing differences between the microbiome communities composition associated with disease development (PERMANOVA, $p = 0.001$)

Development of gingival inflammation was followed by the progression to periodontal bone loss, which was dominated by an adaptive immune response and bone loss (Marchesan et al., 2018). Considering this time course, the microbiome data analysis was stratified based on "clinical phases" of disease, defined as early lesion or gingival inflammation (from 3 days to 6 days) and as periodontitis lesion (from 9 days to 18 days).

The experimental model showed differences in bacterial genera and species abundances from biofilms associated with ligature placement during gingival inflammation and periodontitis development, as can be observed in Figure 4a. Comparison of samples between experimental timelines showed that biofilms harvested at the gingival inflammation stage (3 and 6 days) had lower Shannon diversity indices than the baseline, indicating a decrease in bacterial community diversity within the samples (Figure 4b). This shift was followed by an increased diversity from gingival inflammation to periodontitis (9–18 days). PCoA of unweighted UniFrac showed that samples from baseline (day 0) represented a very distinct community when compared with samples from gingival inflammation and periodontitis stages, which also formed well-defined clusters associated with periodontal clinical diagnosis (Figure 4c). Biofilm community beta diversity from day 0 was significantly different when compared to the community associated with gingival inflammation and periodontitis (Pairwise PERMANOVA, $p = 0.02$ and $p = 0.00$, respectively; Figure 4d). Biofilm community from "gingivitis" samples was also significantly diverse from periodontitis samples (Pairwise PERMANOVA, $p = 0.02$; Figure 4d).

Figure 5a shows a clear distinction among the 20 top ranked species across all clinical diagnosis. Significant species associated with a healthy periodontium were *C. acnes*, *Bacteroides* sp., *B. heparinolyticus*, *A. lwoffii*, *L. fusiformis*, *Rhizobiales* sp., and *Prevotella* sp. Interestingly, the last three species were completely absent in both "gingivitis" and periodontitis statuses. *Staphylococcus* sp. was significantly associated with gingival inflammation with no bone loss, and *Erysipelotrichaceae* was associated with both diseased stages, gingival inflammation, and periodontitis (Figure 5b).

4 | DISCUSSION

This is the first study that reports the oral microbiota shift that occurs during the development and progression of ligature-induced periodontitis. Using a high-throughput method, we found that there were multiple changes in the colonization of the ligature that included anaerobic species. Similar to human disease findings, we identified

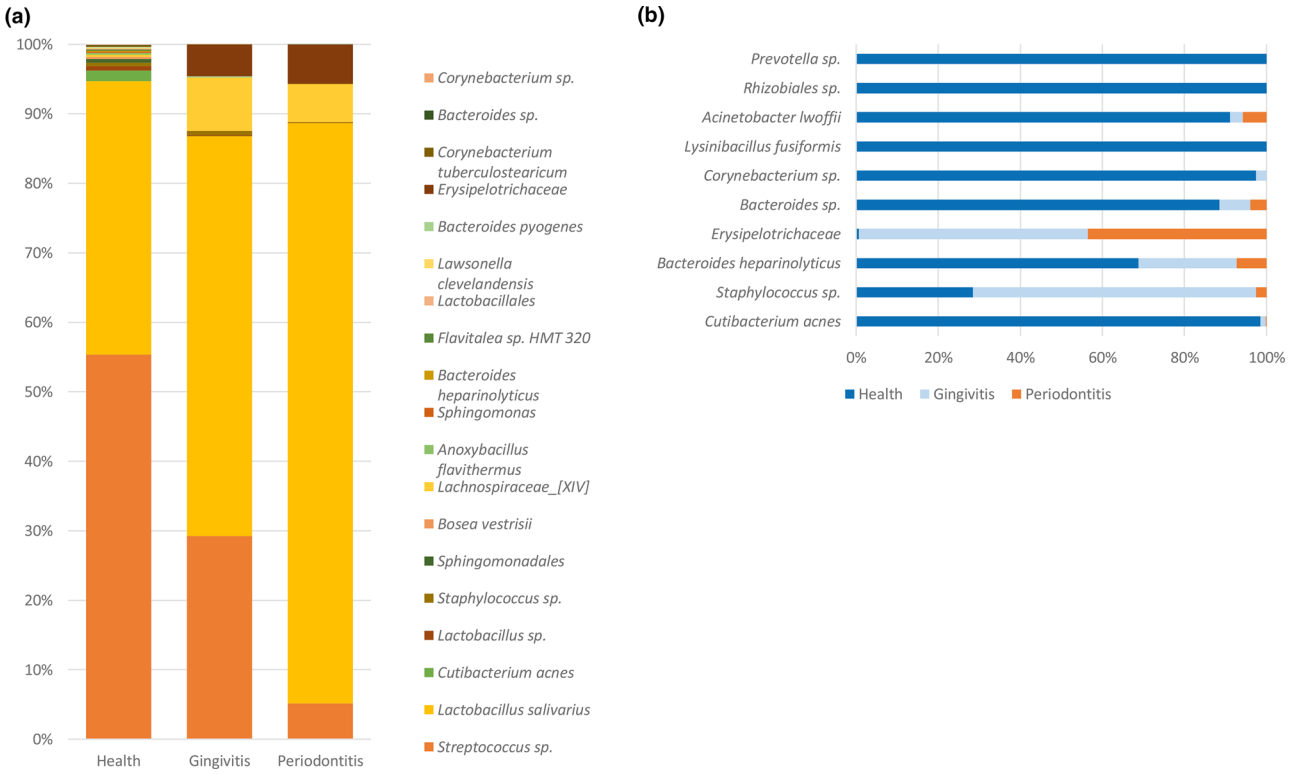

FIGURE 5 Shift of the bacterial microbiome community associated with disease development. (a) Stacked plot for samples' distribution according to clinical diagnosis. For illustrations purposes, only the top 20 genera and species are shown in the plot. The community is represented as 98% in health, 97.7% in gingival inflammation, and 93.5% in periodontitis. (b) Species abundance that significantly changed associated with periodontal disease progression (Mantel–Haensel test, $p < 0.05$, Bonferroni corrected)

an increased microbiota diversity during the transition from gingival inflammation to periodontal bone destruction. These results further support the utilization of the ligature model for microbial shift analysis under different experimental conditions.

Previous studies used a variety of murine models to explore the mechanism of periodontitis and the effectiveness of new treatments. Among these models, the ligature-induced periodontitis model shows host–bacteria interactions, acute alveolar bone loss, and gingival tissue inflammation by 7–9 days (Graves et al., 2008; Marchesan et al., 2018; Abe, Hajishengallis, 2013; Jiao et al., 2013). However, no study has reported a detailed analysis of oral microbiota shifts from health to a dysbiotic state in ligature periodontitis. In this study, we used 16S rRNA gene sequencing of the biofilm microbiota attached to ligatures and identified the presence of seven microbial phyla, with the majority of the composition encompassed by Bacillota and Pseudomonadota. These findings are consistent with other literature reports that have utilized pyrosequencing (Chun et al., 2010) and DGGE (Jiao et al., 2013). In relation to bacterial shift in the biofilm, we identified an increase in Pseudomonadota induced by periodontitis. Previous studies investigated the microbiome shift associated with increases in pathogenicity, using diabetic mice, and verified that higher levels of Pseudomonadota (*Enterobacteriaceae*) and Bacillota (*Enterococcus*, *Staphylococcus*, and *Aerococcus*) were associated with infectious processes, periodontitis, and delayed wound healing (Colombo et al., 2002; Grice et al., 2010; Souto & Colombo, 2008; Vieira Colombo et al., 2016; Demmer et al., 2017). Recent studies show an increase in oral Enterobacteriaceae with ligature-induced periodontitis development, which also agrees with our findings (Kitamoto et al., 2020). Overall, our current study further demonstrated that the Pseudomonadota phylum is positively associated with murine periodontitis progression.

Among the signatures from the microbiome shift time course during biofilm development stages, our data reveal an inversely proportional relationship between a high abundance of *Streptococci* in the early stage versus the progressive increase of *Enterococci* and *Lactobacilli* toward the biofilm maturation. In agreement with previous findings (Sato et al., 2021), we found that some species are associated with gingival health, including *Staphylococcus* and *Corynebacterium*. Interestingly, *Corynebacterium* is also associated with a healthy oral microbiome in humans (Paster et al., 2001). As disease developed in mice, the higher *Streptococcus* prevalence on plaque outset composition was identified in our data corroborated with previous murine studies (Hasegawa et al., 2006, 2010; Jiao et al., 2013). These findings show the importance of this bacteria as a commensal colonizer and early dental biofilm colonizer in the oral cavity, possibly due to its adhesion properties to the hard cementoenamel structures through the secretion of glycoproteins (Teles et al., 2012; Socransky et al., 1977). These findings are translationally consistent with in vivo previous results from our group where nonmature ligature-induced biofilm in an experimental murine model presented enhanced abundance for *Streptococcus gordonii*. In fact, a recent human study revealed that

Streptococcus sp. presence during early onset periodontal disease is consistent among individuals and has the potential to be considered as an early-stage microbial biomarker (Palmer et al., 2017). We identified an increase in levels of *Enterococcus* in the presence of ligature-induced periodontitis, which agrees with previous reports (Sato et al., 2021). The interrelationship between dysbiosis of the subgingival microbiome and periodontitis has been investigated by cohort studies in humans (Deng et al., 2017; Szafranski et al., 2015) and postulated the role of the microbiome on the onset and progression of periodontitis in humans. The red complex pathogen *Porphyromonas gingivalis* was identified as the best marker for periodontitis, followed by *Tannerella* spp., *Treponema* spp., *Fusobacterium_nucleatum_ss_vincentii_HOT_200_V1-2_3*, and *Eubacterium_XI_[G-6]_sp_V1-2_55*. Among the species that showed significant shifts during the time course, *C. acnes* (formerly known as *Propionibacterium acnes*) are gram-positive anaerobic bacilli that are considered commensal bacteria on the skin and, in the oral cavity, have been linked to apical periodontitis in teeth with an existing root canal treatment (Niazi et al., 2010). *Bacteroides heparinolyticus* is a gram-negative anaerobic rod isolated from humans with periodontitis (Okuda et al., 1985). *Corynebacterium dentalis* sp. nov. are gram-positive rods that have been isolated from the dental plaque sample from periodontitis (Benabdelkader et al., 2019). *Lysinibacillus fusiformis* is a gram-positive, rod-shaped bacterium detected for the first time in the root canals. This specie produces extracellular polysaccharides in response to environmental factors (Mahendran et al., 2013). *Acinetobacter lwoffii*, formerly known as *Mima polymorpha* or *Acinetobacter calcoaceticus* var. *lwoffii*, is a nonfermentative gram-negative bacillus frequently associated with respiratory diseases and nosocomial infections due to their rapid development of multidrug resistance, surviving desiccation, and persistence in the environment for long periods of time. This pathogen has also been associated with treatment failure in patients with refractory periodontitis (Colombo et al., 1998; Souto et al., 2014).

Our study identified that ligature-induced periodontitis is associated with microbial dysbiosis, with shifts occurring from health to inflammation, and inflammation to bone destruction. This strengthens the importance of further understanding the microbiota changes that occur with the development of murine periodontitis, which may impact systemic diseases. Murine studies have shown that *P. gingivalis*-induced periodontitis increases both the development and severity of collagen-induced arthritis (Marchesan et al., 2013). Recent data indicate that this is mediated by the oral–gut microbiome (Sato et al., 2017). Importantly, it shows that the oral microbiome has significant impact in the gut microbial composition (Sato et al., 2017). Enterobacteriaceae, a family that we found increased with ligature-induced periodontitis development, was recently shown to accumulate in the gut and lead to colitis after murine periodontitis development (Kitamoto et al., 2020). Therefore, expanding our understanding of the oral microbiome composition is crucial to improve both oral and general health.

In conclusion, this is the first study that reports the shift in microbiome community during periodontitis development, using a combination of the ligature model and "high throughput method." These findings support the utilization of the ligature model for microbial shift analysis under different experimental conditions. Future investigation building on our current study may assist to explore the underlying mechanism between host or environmental factors and microbial dysbiosis in vivo.

ACKNOWLEDGMENTS

The authors would like to thank the following support funding agency/grant numbers T90DE021986 and F32DE026688 (to YJ), K01DE027087 (to JTM), R01AI153265 (to KVS), R01DE023836 (to SO) and the Fulbright/CAPES program finance code 001 (to TA). The UNC Microbiome Core, which is funded in part by the Center for Gastrointestinal Biology and Disease (CGIBD P30 DK034987) and the UNC Nutrition Obesity Research Center (NORC P30 DK056350). The authors would like to thank the late Dr. Steven Offenbacher for his guidance and support during the development of this study.

CONFLICT OF INTEREST

The authors declare no conflict of interest.

DATA AVAILABILITY STATEMENT

The data that supports the findings of this study are available in the supplementary material of this article.

ORCID


Apoena Aguiar Ribeiro https://orcid.org/0000-0001-7702-6178

REFERENCES

Abe, T., & Hajishengallis, G. (2013). Optimization of the ligature-induced periodontitis model in mice. *Journal of Immunological Methods*, *394*, 49–54.

Benabdelkader, S., Boxberger, M., Lo, C. I., Aboudharam, G., La Scola, B., & Fenollar, F. (2019). *Corynebacterium dentalis* sp. nov., a new bacterium isolated from dental plaque of a woman with periodontitis. *New Microbes and New Infections*, *33*, 100625.

Benjamini, Y., & Hochberg, Y. (1995). Controlling the false discovery rate: A practical and powerful approach to multiple testing. *Journal of the Royal Statistical Society: Series B (Methodological)*, *57*, 289–300.

Caporaso, J. G., Kuczynski, J., Stombaugh, J., Bittinger, K., Bushman, F. D., Costello, E. K., Fierer, N., Peña, A. G., Goodrich, J. K., Gordon, J. I., Huttley, G. A., Kelley, S. T., Knights, D., Koenig, J. E., Ley, R. E., Lozupone, C. A., McDonald, D., Muegge, B. D., Pirrung, M., … Knight, R. (2010). QIIME allows analysis of high-throughput community sequencing data. *Nature Methods*, *7*(5), 335–336. https://doi.org/10.1038/nmeth.f.303

Chun, J., Kim, K. Y., Lee, J. H., & Choi, Y. (2010). The analysis of oral microbial communities of wild-type and toll-like receptor 2-deficient mice using a 454 GS FLX Titanium pyrosequencer. *BMC Microbiology*, *10*, 101.

Colombo, A. P., Haffajee, A. D., Dewhirst, F. E., Paster, B. J., Smith, C. M., Cugini, M. A., & Socransky, S. S. (1998). Clinical and microbiological features of refractory periodontitis subjects. *Journal of Clinical Periodontology*, *25*, 169–180.

Colombo, A. P., Teles, R. P., Torres, M. C., Souto, R., Rosalem, W. J., Mendes, M. C., & Uzeda, M. (2002). Subgingival microbiota of Brazilian subjects with untreated chronic periodontitis. *Journal of Periodontology*, *73*, 360–369.

Demmer, R. T., Breskin, A., Rosenbaum, M., Zuk, A., LeDuc, C., Leibel, R., Paster, B., Desvarieux, M., Jacobs, D. R., Jr., & Papapanou, P. N. (2017). The subgingival microbiome, systemic inflammation and insulin resistance: The oral infections, glucose intolerance and insulin resistance study. *Journal of Clinical Periodontology*, *44*(3), 255–265.

Deng, K., Ouyang, X. Y., Chu, Y., & Zhang, Q. (2017). Subgingival microbiome of gingivitis in Chinese undergraduates. *The Chinese Journal of Dental Research*, *20*(3), 145–152.

Edwards, U., Rogall, T., Blocker, H., Emde, M., & Bottger, E. C. (1989). Isolation and direct complete nucleotide determination of entire genes. Characterization of a gene coding for 16S ribosomal RNA. *Nucleic Acids Research*, *17*(19), 7843–7853.

Graves, D. T., Fine, D., Teng, Y.-T. A., Van Dyke, T. E., & Hajishengallis, G. (2008). The use of rodent models to investigate host-bacteria interactions related to periodontal diseases. *Journal of Clinical Periodontology*, *35*, 89–105.

Grice, E. A., Snitkin, E. S., Yockey, L. J., Bermudez, D. M., N. Comparative Sequencing Program. Liechty, K. W., & Segre, J. A. (2010). Longitudinal shift in diabetic wound microbiota correlates with prolonged skin defense response. *Proceedings of the National Academy of Sciences of the United States of America*, *107*(33), 14799–14804. https://doi.org/10.1073/pnas.1004204107

Griffen, A. L., Beall, C. J., Campbell, J. H., Firestone, N. D., Kumar, P. S., Yang, Z. K., Podar, M., & Leys, E. J. (2012). Distinct and complex bacterial profiles in human periodontitis and health revealed by 16S pyrosequencing. *The ISME Journal*, *6*, 1176–1185.

Hajishengallis, G., Lamont, R. J., & Graves, D. T. (2015). The enduring importance of animal models in understanding periodontal disease. *Virulence*, *6*, 229–235.

Hajishengallis, G., & Lamont, R. J. (2016). Dancing with the stars: How choreographed bacterial interactions dictate nososymbiocity and give rise to keystone pathogens, accessory pathogens, and pathobionts. *Trends in Microbiology*, *24*, 477–489.

Hasegawa, M., Yang, K., Hashimoto, M., Park, J. H., Kim, Y. G., Fujimoto, Y., Nuñez, G., Fukase, K., & Inohara, N. (2006). Differential release and distribution of Nod1 and Nod2 immunostimulatory molecules among bacterial species and environments. *Journal of Biological Chemistry*, *281*(39), 29054–29063. https://doi.org/10.1074/jbc.M602638200

Hasegawa, M., Osaka, T., Tawaratsumida, K., Yamazaki, T., Tada, H., Chen, G. Y., Tsuneda, S., Núñez, G., & Inohara, N. (2010). Transitions in oral and intestinal microflora composition and innate immune receptor-dependent stimulation during mouse development. *Infection and Immunity*, *78*(2), 639–650. https://doi.org/10.1128/IAI.01043-09

Hochberg, Y., & Benjamini, Y. (1990). More powerful procedures for multiple significance testing. *Statistics in Medicine*, *9*(7), 811–818. https://doi.org/10.1002/sim.4780090710

Jiao, Y., Hasegawa, M., & Inohara, N. (2014). The role of oral pathobionts in dysbiosis during periodontitis development. *Journal of Dental Research*, *93*, 539–546.

Jiao, Y., Darzi, Y., Tawaratsumida, K., Marchesan, J. T., Hasegawa, M., Moon, H., Chen, G. Y., Núñez, G., Giannobile, W. V., Raes, J., & Inohara, N. (2013). Induction of bone loss by pathobiont-mediated Nod1 signaling in the oral cavity. *Cell Host & Microbe*, *13*(5), 595–601. https://doi.org/10.1016/j.chom.2013.04.005

Jones, R. B., Zhu, X., Moan, E., Murff, H. J., Ness, R. M., Seidner, D. L., Sun, S., Yu, C., Dai, Q., Fodor, A. A., Azcarate-Peril, M. A., & Shrubsole, M. J. (2018). Inter-niche and inter-individual variation in gut microbial community assessment using stool, rectal swab, and mucosal samples. *Scientific Reports*, *8*(1), 4139.

Kitamoto, S., Nagao-Kitamoto, H., Jiao, Y., Gillilland, M. G., 3rd, Hayashi, A., Imai, J., Sugihara, K., Miyoshi, M., Brazil, J. C., Kuffa, P., Hill, B. D., Rizvi, S. M., Wen, F., Bishu, S., Inohara, N., Eaton, K. A., Nusrat, A., Lei, Y. L., Giannobile, W. V., & Kamada, N. (2020). The intermucosal connection between the mouth and gut in commensal pathobiont-driven colitis. *Cell*, *182*(2), 447.e14–462.e14.

Mahendran, S., Vijayabaskar, P., Saravanan, S., Anandapandian, K. T. K., & Shank, T. (2013). Structural characterization and biological activity of exopolysaccharide from *Lysinibacillus fusiformis*. *African Journal of Microbiology Research*, *7*, 4629–4639.

Marchesan, J., Girnary, M. S., Jing, L., Miao, M. Z., Zhang, S., Sun, L., Morelli, T., Schoenfisch, M. H., Inohara, N., Offenbacher, S., & Jiao, Y. (2018). An experimental murine model to study periodontitis. *Nature Protocols*, *13*(10), 2247–2267.

Marchesan, J., Jiao, Y., Schaff, R. A., Hao, J., Morelli, T., Kinney, J. S., Gerow, E., Sheridan, R., Rodrigues, V., Paster, B. J., Inohara, N., & Giannobile, W. V. (2016). TLR4, NOD1 and NOD2 mediate immune recognition of putative newly identified periodontal pathogens. *Molecular Oral Microbiology*, *31*, 243–258.

Marchesan, J. T., Morelli, T., Lundy, S. K., Jiao, Y., Lim, S., Inohara, N., Nunez, G., Fox, D. A., & Giannobile, W. V. (2012). Divergence of the systemic immune response following oral infection with distinct strains of *Porphyromonas gingivalis*. *Molecular Oral Microbiology*, *27*(6), 483–495.

Marchesan, J. T., Gerow, E. A., Schaff, R., Taut, A. D., Shin, S. Y., Sugai, J., Brand, D., Burberry, A., Jorns, J., Lundy, S. K., Nuñez, G., Fox, D. A., & Giannobile, W. V. (2013). *Porphyromonas gingivalis* oral infection exacerbates the development and severity of collagen-induced arthritis. *Arthritis Research & Therapy*, *15*(6), R186.

Niazi, S. A., Clarke, D., Do, T., Gilbert, S. C., Mannocci, F., & Beighton, D. (2010). *Propionibacterium acnes* and *Staphylococcus epidermidis* isolated from refractory endodontic lesions are opportunistic pathogens. *Journal of Clinical Microbiology*, *48*(11), 3859–3869.

Nociti, F. H., Jr., Casati, M. Z., & Duarte, P. M. (2015). Current perspective of the impact of smoking on the progression and treatment of periodontitis. *Periodontology 2000*, *67*, 187–210.

Okuda, K., Kato, T., Shiozu, J., Takazoe, I., & Nakamura, T. (1985). *Bacteroides heparinolyticus* sp. nov. isolated from humans with periodontitis. *International Journal of Systematic Bacteriology*, *35*, 438–442.

Paes Batista da Silva, A., Barros, S. P., Moss, K., Preisser, J., Marchesan, J. T., Ward, M., & Offenbacher, S. (2016). Microbial profiling in experimentally induced biofilm overgrowth among patients with various periodontal states. *Journal of Periodontology*, *87*, 27–35.

Palmer, R. J., Jr., Shah, N., Valm, A., Paster, B., Dewhirst, F., Inui, T., & Cisar, J. O. (2017). Interbacterial adhesion networks within early oral biofilms of single human hosts. *Applied and Environmental Microbiology*, *83*(11), e00407–17.

Paster, B. J., Boches, S. K., Galvin, J. L., Ericson, R. E., Lau, C. N., Levanos, V. A., Sahasrabudhe, A., & Dewhirst, F. E. (2001). Bacterial diversity in human subgingival plaque. *Journal of Bacteriology*, *183*, 3770–3783.

Sanz, M., Ceriello, A., Buysschaert, M., Chapple, I., Demmer, R. T., Graziani, F., Herrera, D., Jepsen, S., Lione, L., Madianos, P., Mathur, M., Montanya, E., Shapira, L., Tonetti, M., & Vegh, D. (2018). Scientific evidence on the links between periodontal diseases and diabetes: Consensus report and guidelines of the joint workshop on periodontal diseases and diabetes by the International Diabetes Federation and the European Federation of Periodontology. *Journal of Clinical Periodontology*, *45*, 138–149.

Sato, K., Yamazaki, K., Kato, T., Nakanishi, Y., Tsuzuno, T., Yokoji-Takeuchi, M., Yamada-Hara, M., Miura, N., Okuda, S., Ohno, H., & Yamazaki, K. (2021). Obesity-related gut microbiota aggravates alveolar bone destruction in experimental periodontitis through elevation of uric acid. *mBio*, *12*(3), e0077121.

Sato, K., Takahashi, N., Kato, T., Matsuda, Y., Yokoji, M., Yamada, M., Nakajima, T., Kondo, N., Endo, N., Yamamoto, R., Noiri, Y., Ohno, H., & Yamazaki, K. (2017). Aggravation of collagen-induced arthritis by orally administered *Porphyromonas gingivalis* through modulation of the gut microbiota and gut immune system. *Science Reports*, *7*, 6955.

Socransky, S. S., Manganiello, A. D., Propas, D., Oram, V., & van Houte, J. (1977). Bacteriological studies of developing supragingival dental plaque. *Journal of Periodontal Research*, *12*(2), 90–106.

Souto, R., & Colombo, A. P. (2008). Prevalence of *Enterococcus faecalis* in subgingival biofilm and saliva of subjects with chronic periodontal infection. *Archives of Oral Biology*, *53*(2), 155–160. https://doi.org/10.1016/j.archoralbio.2007.08.004

Souto, R., Silva-Boghossian, C. M., & Colombo, A. P. (2014). Prevalence of *Pseudomonas aeruginosa* and *Acinetobacter* spp. in subgingival biofilm and

saliva of subjects with chronic periodontal infection. *Brazilian Journal of Microbiology*, *45*(2), 495–501.

Swanson, K. V., Girnary, M., Alves, T., Ting, J. P., Divaris, K., Beck, J., Pucinelli, C. M., da Silva, R. A. B., Uyan, D., Wilson, J. E., Seaman, W. T., Webster-Cyriaque, J., Vias, N., Jiao, Y., Cantley, L., Marlier, A., Arnold, R. R., & Marchesan, J. T. (2022). Interferon activated gene 204 (**I**fi204) protects against bone loss in experimental periodontitis. *Journal of Periodontology*, *93*(9), 1366–1377.

Szafranski, S. P., Wos-Oxley, M. L., Vilchez-Vargas, R., Jáuregui, R., Plumeier, I., Klawonn, F., Tomasch, J., Meisinger, C., Kühnisch, J., Sztajer, H., Pieper, D. H., & Wagner-Döbler, I. (2015). High-resolution taxonomic profiling of the subgingival microbiome for biomarker discovery and periodontitis diagnosis. *Applied and Environmental Microbiology*, *81*(3), 1047–1058.

Teles, F. R., Teles, R. P., Uzel, N. G., Song, X. Q., Torresyap, G., Socransky, S. S., & Haffajee, A. D. (2012). Early microbial succession in redeveloping dental biofilms in periodontal health and disease. *Journal of Periodontal Research*, *47*(1), 95–104.

Teles, F., Wang, Y., Hajishengallis, G., Hasturk, H., & Marchesan, J. T. (2021). Impact of systemic factors in shaping the periodontal microbiome. *Periodontology 2000*, *85*(1), 126–160.

Thompson, A. L., Monteagudo-Mera, A., Cadenas, M. B., Lampl, M. L., & Azcarate-Peril, M. A. (2015). Milk- and solid-feeding practices and day-care attendance are associated with differences in bacterial diversity, predominant communities, and metabolic and immune function of the infant gut microbiome. *Frontiers in Cellular and Infection Microbiology*, *5*, 5.

Vieira Colombo, A. P., Magalhães, C. B., Hartenbach, F. A., Martins do Souto, R., & Maciel da Silva-Boghossian, C. (2016). Periodontal-disease-associated biofilm: A reservoir for pathogens of medical importance. *Microbial Pathogenesis*, *94*, 27–34.

SUPPORTING INFORMATION

Additional supporting information can be found online in the Supporting Information section at the end of this article.

How to cite this article: Ribeiro, A. A., Jiao, Y., Girnary, M., Alves, T., Chen, L., Farrell, A., Wu, D., Teles, F., Inohara, N., Swanson, K. V., & Marchesan, J. T. (2022). Oral biofilm dysbiosis during experimental periodontitis. *Molecular Oral Microbiology*, *37*, 256–265. https://doi.org/10.1111/omi.12389